# Surface Estimation of a Pedestrian Walk for Outdoor Use of Power Wheelchair Based Robot

Abdul Attayyab Khan[1], S. Riaz un Nabi[2], Jamshed Iqbal[3]

[1.] Department of Electrical Engineering, King Faisal University, Kingdom of Saudi Arabia
[2.] Electronic Engineering Department, NED UET, Karachi, Pakistan
[3.] Department of Electrical Engineering, COMSATS Institute of Information Technology, Islamabad, Pakistan
jamshed.iqbal@comsats.edu.pk

**Abstract:** In mobile robotics, surface estimation and object recognition play vital role in navigation and control. This research presents a normal vector estimation method of a surface using Delaunay tessellation. The proposed strategy is an expansion of previously developed Continuous Nearest Neighbor Algorithm, underlining the trade-off between filtering and quality of input data. Initially, the 3D data points are segmented through a threshold process. The normal vectors are then determined based on an averaging method of centroids on Delaunay tessellation. Moreover, two similarity measures (vector angle and Euclidean distance) are considered for surface estimation of a pedestrian walk. Output from the Delaunay triangulation provides information for surface estimation. Results show that the proposed strategy has a great potential to be used for surface estimation in robotics.

[Abdul Attayyab Khan, S. Riaz un Nabi, Jamshed Iqbal. **Surface Estimation of a Pedestrian Walk for Outdoor Use of Power Wheelchair Based Robot**. *Life Sci J* 2013; 10(3): 1697-1704]. (ISSN: 1097-8135). http://www.lifesciencesite.com 255

**Keywords:** Surface estimation; Service robotics; Assistive robots

## 1. Introduction

Technological advancements in robotics and associated technologies have helped to bring about and corroborate the maturity of the field [1]. From a largely pre-eminent industrial focus, robotics has now expeditiously opened out into the challenges of human world. The up-coming era of robots presume safety and co-op in different application scenarios at homes, workplaces and communities, providing support in services, health care, manufacturing and assistance [2]. In robot design, there are associated key factors that involve several aspects to be integrated in various disciplines of robotics [3]. Among those factors, robot kinematics, signal analysis, 3D surface estimation and recognition play a vital role in realizing the overall system. 3D data handling from the sensors in Visual Servoing (VS) for object detection or surface recognition relies on analysis of sensor response [4].

Challenges like navigation, Simultaneous Localization and Mapping (SLAM) and obstacle avoidance have been successfully addressed and overcome for structured indoor environment. However, more work needs to be done for outdoor environments to meet the challenges, raised due to crucial and sensitive nature of constraints imposed by such environments [5]. For this high-level task, object recognition, factual awareness and interpretation of objects in the environment serve as imperatives and prerequisites [6]. The problem that needs to be addressed is to develop techniques that can be used to design a robust algorithm enabling a mobile robot, or a wheelchair, to drive safely in outdoor environments [7]. There is no exaggeration in stating that surface estimation and obstacle avoidance are essential primitives in mobile robotics in general. Precisely, enabling a wheelchair based robot to operate in an outdoor environment is a non-trivial and challenging task. It is required to make a wheelchair move around under its own power and function semi-autonomously. Thus it can be operated under all reasonable and challenging conditions without requiring resource allocation to a human operator, considering all operating safety regulations.

The goal of this research is to estimate the pedestrian surface and analyze sensor response in outdoor environment, for surface estimation of a pedestrian walk. Range data is actually a prerequisite in object recognition, surface estimation and to have better understanding of environment [8]. To control the movement of a dynamic system for VS, it is required to use the information provided by a vision sensor [9]. The power wheelchair used in this research is equipped with Fotonic B70 3D Laser Range Finder (LRF), a laptop computer, and Xsens Inertial Measurement Unit (IMU). The LRF is used as a main navigation sensor for surface estimation and detection of a flat surface in front of the power wheelchair. Moreover, IMU package (in sensor fusion with the laser sensor), is used for dead reckoning and is needed for real-time estimation of Euler angles, acceleration (linear), velocity (angular, linear), rotation matrix etc.

The remaining of the paper is structured as follows: Section 2 explains mapping, segmentation and reconstruction of 3D range data from the LRF. Section 3 introduces two different methods for surface estimation used in this research. Section 4 explains the coordinate transformation for updating the position of the wheelchair. Experimental results are discussed in Section 5 and finally Section 6 comments on conclusion.

## 2. 3D Data Mapping

The 3D range data obtained from LRF is mapped to correspond with the set of 3D values of the surface in real world [10]. 3D range data permit to recognize objects and to estimate surfaces in indoor as well as in outdoor environments.

**3D Range Data:** Considering set of *n* points to examine the surface having points $P_i = \{p_{(i,1)}, \cdots, p_{(i,n}$ within one scan which further needs to be represented in data matrix $P = [p_1, \ldots, p_n$ where $p_i = [p_{ix}, p_{iy}, p_{iz}$ represents 3D coordinates of a point. Moreover, it is required to estimate normal vector $n_i = [n_{ix}, n_{iy}, n_{iz}$ from its nearest neighbourhood $Q_i = [q_{i1}, q_{i2}, \cdots, q_{ik}$ and $Q_i^+ = [q_{i1}, q_{i2}, \cdots, q_{ik}$, which contain all points in neighborhood of the point [8].

**Segmentation of Range Data:** Scientific literature reports various methods for range data segmentation [11, 12]. Examining the 3D response from LRF, it is required to segment the data set [13]. So the portion containing the error points needs to be segmented out from the whole scan. For this purpose, we proposed and implemented a technique that works on depth component (z) of the range data. The original z-component of the image gives the segmented image of the pedestrian walk of the image [14]. All the points where $z_{mec}$ is less than $z_{mean}$ are considered for the new segmented image. Thus, from here we get the segmented surface points denoted by $P_S$ that are free from error with coordinate $P_S = [P_{S_x}, P_{S_y}, P_{S_z}$. Figure 1(a) and (b) shows the real image from an ordinary camera and the active brightness image from the laser sensor respectively. Figure 1(c) illustrates 3D depth data from the sensor where the error points in scan and edge between pedestrian walk and road are depicted. The point cloud response of laser sensor is shown in Figure 1(d). Figure 2 presents the segmented pedestrian surface [15, 16].

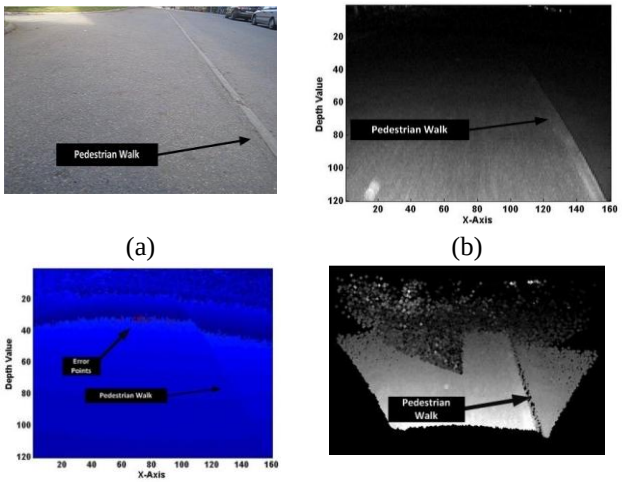


(a) (b)

(c) (d)

Figure 1. Pedestrian surface (a) Ordinary camera image (b) Active brightness image with pedestrian walk curbstone marked (c) Depth image (d) Point cloud where also no detects and noisy points are visible to the upper left

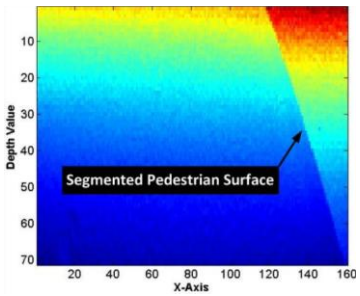


Figure 2. Distance image where distances are mapped to colors

**Reconstruction of Range Data:** After segmentation of 3D data, it is required to reconstruct it considering three coordinates x, y, and z. Figure 3 shows point cloud of the reconstructed 3D surface.

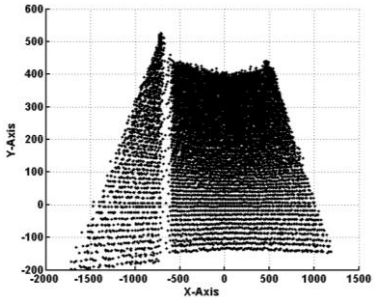


Figure 3. 3D point cloud

The reconstructed surface segmented data is presented in Figure 4 (a) while (b) shows the 3D point cloud. The single scan in Fig. 4 (c) contains outliers in the data points and needs to be rectified

before finding neighborhood and . Fig. 5 (a) and (c) illustrate two surfaces before filtration. As shown, the surfaces are not uniform and thus are not suitable for normal vector estimation thereby requiring filtration of the surface data [17]. The 3D data obtained is filtered with a median filter. It helps to get rid of uneven distribution of points on the surface. Figure 5 (b) and (d) shows the corresponding filtered 3D surfaces.

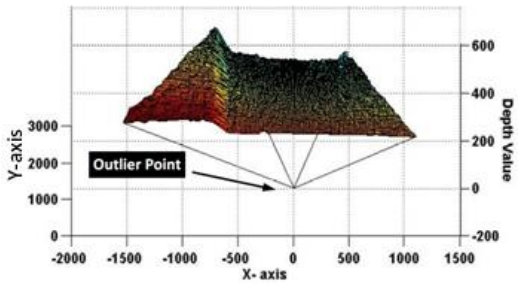


(a)

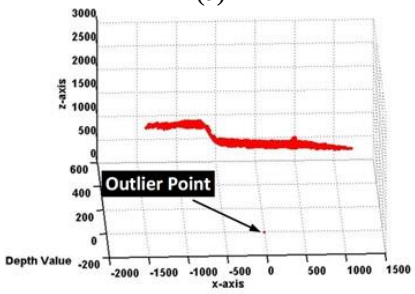


(b)

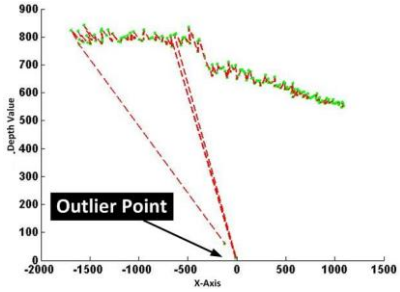


(c)

Figure 4. Outlier Points in 3D Scan
(a) 3D surface showing outlier (b) 3D point cloud
(c) XY view of single scan showing outlier

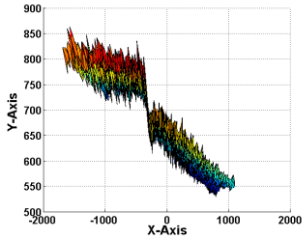


(a)

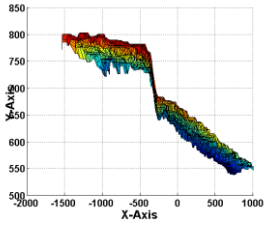


(b)

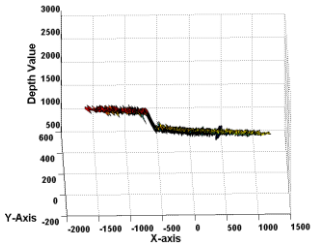


(c)

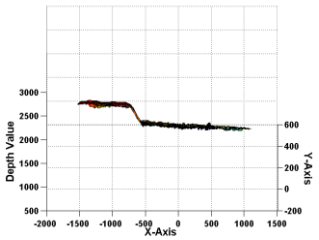


(d)

Figure 5. Surface 1 and 2:
(a) and (c) before filtration
(b) and (d) after filtration

### 3. Surface Estimation

In the present work, following two techniques have been adopted for surface estimation:

- Normal vector estimation (Delaunay triangulation).
- Agglomerative hierarchical clustering of 3D points (Mahalanobis distance).

**Delaunay Triangulation:** From set of 3D segmented data points, the Delaunay triangulation has been created, where circumcircle associated with each triangle contains no other points in its interior [18]. Consider the Delaunay triangulation $(d_t)$ of the segmented points $(P_S)$ with triangulation $d_{tr} = \{d_{tr1}, d_{tr2}, \ldots, d_{trn}\}$, where $d_{tr_i} = \left[d_{tr_{ix}}, d_{tr_{iy}}, d_{tr_{iz}}\right]$ is a set of 3D coordinates of triangle vertices. Figure 6 shows the result of Delaunay triangulation experiment.

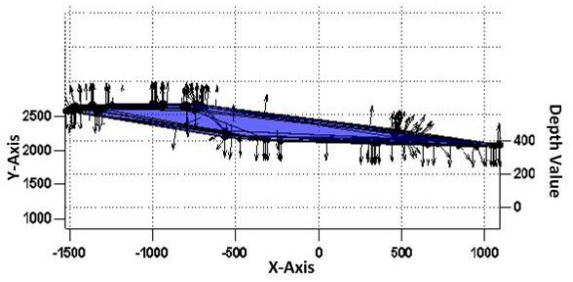


(a)

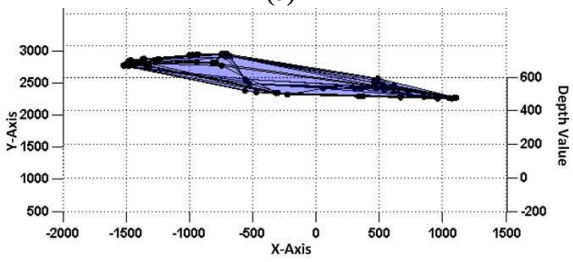


(b)

Figure 6. Delaunay triangulation with sensor at 4
(a) With normal vectors
(b) Without normal vectors

The 3D triangulation coordinates $d_{tri}$ are used to find the center of the triangles formed from Delaunay triangulation $d_{tr}$ . Assume that the coordinates of the vertices of a triangle denoted as $d_{tr1} = \{d_{tr_{1x}}, d_{tr_{1y}}, d_{tr_{1z}}\}$, $d_{tr2} = \{d_{tr_{2x}}, d_{tr_{2y}}, d_{tr_{2z}}\}$ and $d_{tr3} = \{d_{tr_{3x}}, d_{tr_{3y}}, d_{tr_{3z}}\}$ are used to find the center of the triangle. The normal vectors can now be estimated on the center points of the triangles. These will be further used as the normal vectors on point $P_S$. Fig. 7(a) and (b) present the 2D and 3D views of normal vector estimation on the center of the Delaunay triangles respectively, where the portions highlighted are the edges joined with the points showing neighbors of point $P_1$. Edge attachment technique has been then adopted, where every query point $q$ in the triangulation and its neighbors are examined based on edges in the triangulation. The vertices of the edges which represent the vertex coordinates of the triangles are the neighbors of the query point. As shown in Fig. 7(a), that the edges attached with the point $p_1$ connects it to neighboring points $p_3$ , $p_4$ , $p_5$ and $p_6$ . Moreover, the method to find normal vector on the query point is to average normal vectors to the triangles formed by the combination of its neighbors.

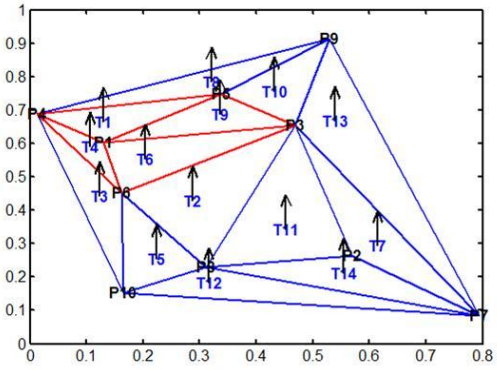


(a)

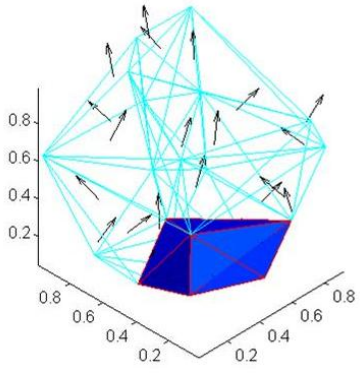

(b)

Figure 7. Delaunay triangulation
(a) 2D view (b) 3D view

Two measures have been considered for an estimated normal vector (. These include angle between the normal vectors ( ) and Euclidean distance measure (. The next step after the vector estimation is to find the angle between the vectors which helps to understand the similarity of the normal vectors. The angle between the vectors can be found using (1).

$$\theta_a(p_i, p_j) = cos^{-1}\left(\frac{p_i \cdot p_j}{\|p_i\|\|p_j\|}\right) \quad (1)$$

The second measure, Euclidean similarity gives the distance between points $p_i$ and $p_j$ belonging to same set of 3D points. Equation (2) gives this measured distance.

$$d_e(p_i, p_j) = \|p_i - p_j\| \quad (2)$$

**Agglomerative Hierarchical Clustering:** Mahalanobis distance is another measure used for surface estimation [19] and robot navigation in outdoor environment [20]. Based on 3D information from Laser sensor and points $p_1$ ,…, $p_n$ of $P = [p_1, \ldots, p_n]^T$, the distance between the points is determined using ward linkage method [5] to obtain the clustered data. To compute the measure of similarity between two surfaces $s_1$ and $s_2$ belonging to same data set of 3D points, Mahalanobis distance between two points is determined by (3)

$$d_M(p_i, p_j) = \sqrt{(p_i - p_j)^T S^{-1}(p_i - p_j)} \quad (3)$$

Where S is the covariance matrix of 3D points and can be given as (4). Figure 8(a) and (b) shows the clustered data set of all 3D points from Mahalanobis distance.

$$S = \frac{1}{N-1} P_i^T P_i \quad (4)$$

Where $P_i$ is a matrix composed from coordinates of the points of a single scan.

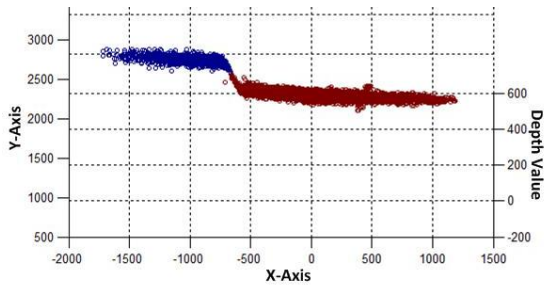


(a)

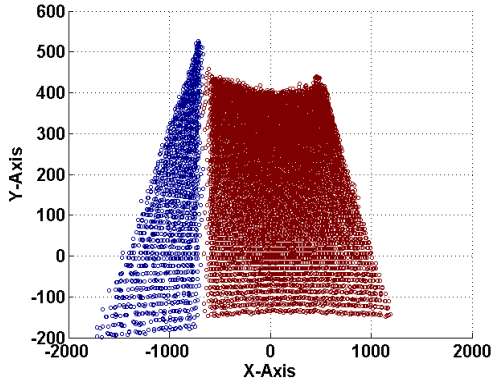


(b)

Figure 8. Clustered 3D points of estimated surface
(a) Actual view (b) 2D view

## 4. Coordinate Transformation

The transformation of the coordinate system is one of the essential steps that helps to update the position of a wheelchair based on the transformation between the pose of the wheelchair and the Laser range measurements. Apart from surface estimation, localization of the wheelchair data association is another important step that affirms the validity of the extracted data to associate it with known features in world coordinates. To represent the position and orientation of the wheelchair, it is required to define the coordinate system with respect to LRF. For this purpose, transformation of IMU and the wheelchair coordinates need to be carried out for getting the orientation of the wheelchair with respect to LRF. The overall transformation of coordinate frames is shown in Figure 9 where the Xsens IMU and wheelchair coordinates are transformed into LRF coordinate system to finally perceive it in world coordinate system. Transformation of IMU to LRF is shown in Figure 10(a) while (b) shows the transformation of wheelchair coordinates into LRF coordinates.

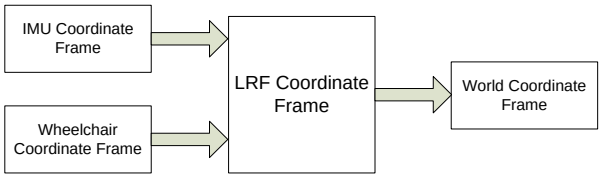


Figure 9. Coordinate transformation

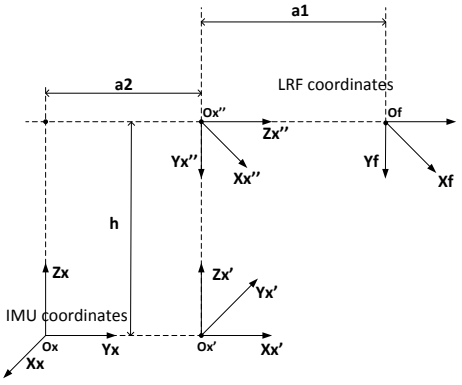


(a)

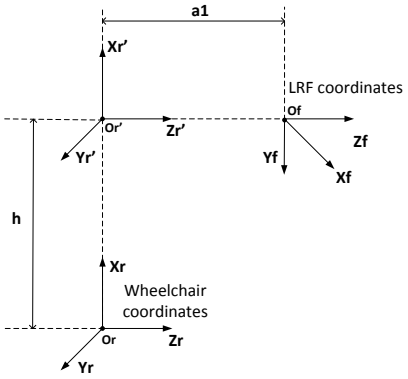


(b)

Figure 10. Coordinate transformation:
(a) Xsens IMU to LRF (b) Wheelchair to LRF

## 5. Experimental Results

To access the efficiency of the presented estimation methods, two different scenarios involving multiple data sets have been taken. These are:

- Moving down along a pedestrian walk.
- Moving up along a pedestrian walk.

**Experimental Setup and Data Collection:** A Commercial off the shelf power wheelchair (Permobil C350), on which all the equipment has been mounted was used to record data. The equipment includes a laser range camera (Fotonic B70), an IMU (XSens MTi-G) and a dedicated laptop and a computer USB interface to the power wheelchair. The IMU package provides orientation of the wheelchair along with acceleration, Euler angles (roll, pitch and yaw) and rotation matrix. Figure 11 shows the wheelchair equipped with LRF. Data recorded with LRF and IMU fused together in a single data structure.

Figure 11. Permobil C350 Wheelchair

**Laser Sensor Data:** The first experiment has been carried out by placing the laser sensor at an angle of $90^{\circ}$ with respect to the base of the wheelchair. For second experiment, the sensor placement has been changed to 45°. Results have demonstrated that placing the sensor at 45° helps to achieve more useful data (surface) and reduced unnecessary data (environment) in contrast with sensor placement at 90°. Figures 12 and 13 respectively show corresponding data with 90° and 45° angles taken from the sensor with their clustered data, point cloud, surface diagram and single scan. The reconstructed segmented surface with 45° sensor angle also gives less error points and outliers present in the scan.

**Surface Estimation:** Clustering through Mahalanobis distances permits surface estimation as illustrated in Figures 12 (d) and 13 (c). Figures 12 (a) and 13 (a) show the simple 2D point cloud for 90° and 45° cases respectively while Figures 12 (c) and 13 (c) present the corresponding 2D view of surfaces after the clustering process. The cluster boundaries can assist in providing the boundaries of the surface on which the wheelchair can drive safely.

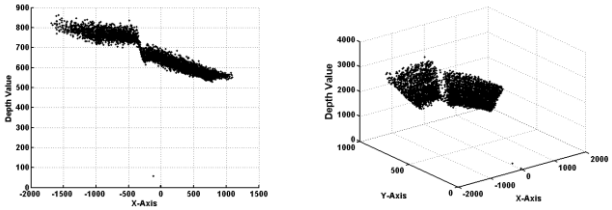


(a) (b)

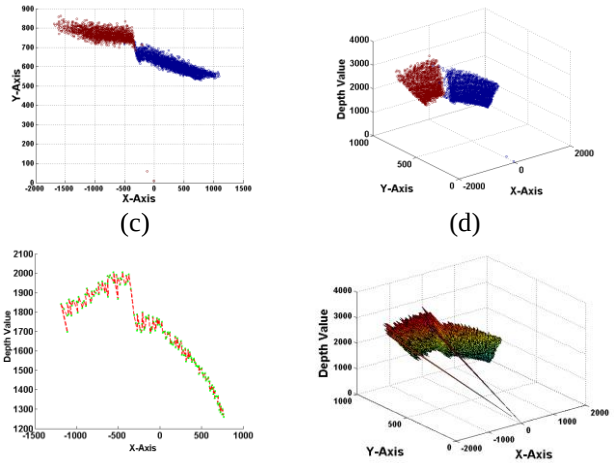


(c) (d)

(e) (f)

Figure 12. Laser sensor adjustment at 90°
(a) 2D view point cloud (b) 3D view point cloud
(c) 2D view data clustering (d) 3D view data clustering
(e) 2D view single scan (f) 3D view of surface

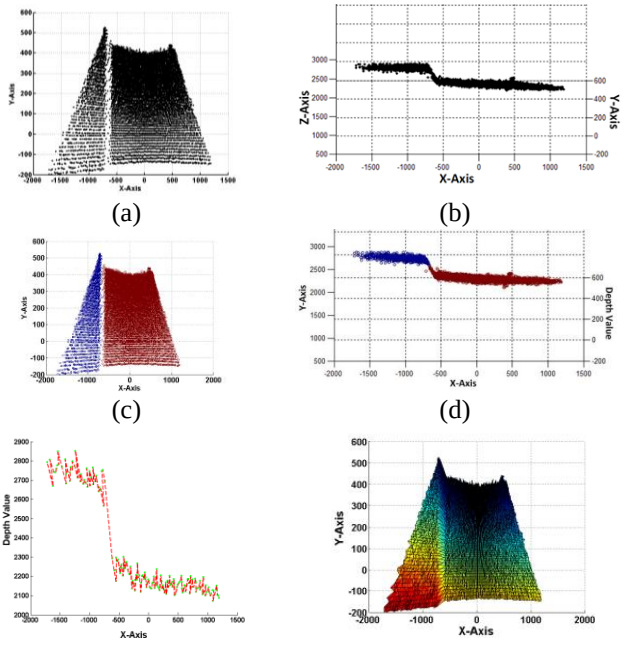


(a) (b)

(c) (d)

(e) (f)

Figure 13. Laser sensor adjustment at 45°
(a) 2D view point cloud (b) 3D view point cloud
(c) 2D view data clustering (d) 3D view data clustering
(e) 3D view single scan (f) 2D view of surface

Moreover, Euclidean similarity ($d_e$) and angular similarity ($\theta_a$) (Section 3) between the vectors are other indicators of surface estimation as shown in Figure 14. Implementation of the proposed approach on the real wheel chair based robot has demonstrated the successful estimation of a pedestrian surface. Results of Delaunay triangulation

method ($\theta_a$) provide estimation of the pedestrian walk as illustrated in Figure 15.

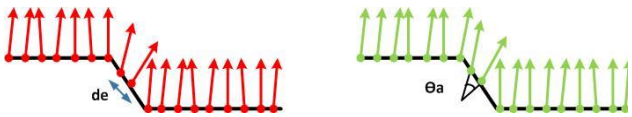


Figure 14. Euclidean $d_e$ and Angular $\theta_a$

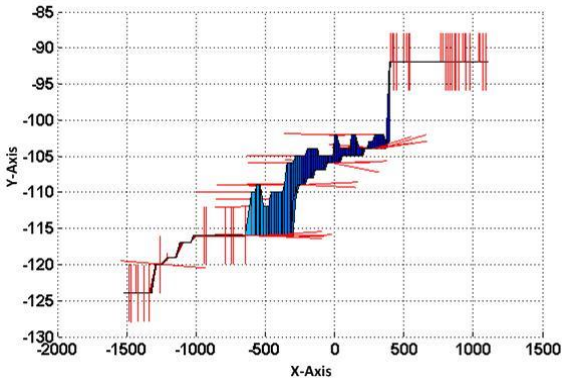


Figure 15. Surface vectors

## 5. Conclusion

This research proposes strategy for surface estimation of a pedestrian walk to assist mobility of a power wheel chair based robot semi-autonomously in an outdoor environment using 3D Laser data. The designed algorithm is based on normal vector estimation and Mahalanobis distance. The quality of surface estimation depends on different factors like quality of 3D data and orientation of the laser sensor which affects the number of data points for surface estimation.

## 6. Future Work

Considering the information from surface estimation and data clustering, continuous sequence of cluster boundaries can be used in designing the suitable controller to navigate through drivable path. Landmarks can also be used for localization. The LRF data becomes the basis of design of the navigation loop. Velocity and steering angle information from IMU help to estimate its position and orientation in world coordinate frame. The presented algorithmic technique can successfully be tested using a real platform, and expected to have potential in robotics. Related research which would certainly be beneficial for people having reduced mobility includes integration of wheelchair with a robotic hand exoskeleton [21-27] and control of wheelchair using brain signals [28].

**Acknowledgements:** Special thanks to Umeå University, Sweden for providing resources and technical support for this research.

**Corresponding Author:**
Abdul Attayyab Khan
Lecturer, Department of Electrical Engineering,
King Faisal University (KFU),
Kingdom of Saudia Arabia (KSA)
E-mail: akhan@kfu.edu.sa

## REFERENCES

[1] Robin R. Murphy, "*Introduction to AI Robotics*", A Bradford Book, MIT Press Cambridge, Massachusetts, 2000, pp. 3-5.
[2] K. Georgiev and R. Lakaemper, "3D data classification based on mid-level geometric features", IEEE International Conference on Advanced Robotics (ICAR). 2011, pp. 310–315.
[3] K. Klasing, D. Wollherr and M. Buss, "Clustering method for efficient segmentation of 3D laser data", IEEE International Conference on Robotics and Automation (ICRA), 2008, pp. 4043 – 4048.
[4] A. Dame and E. Marchand, "Entropy-based visual servoing", IEEE International Conference on Robotics and Automation (ICRA), 2009, pp. 707 – 713.
[5] G. Grudic and J. Mulligan, "Outdoor path labeling using polynomial Mahalanobis distance", Robotics: Science and Systems (RSS), 2006.
[6] S. S. Fukusima, J. M. Loomis and J.A. Da Silva, "Visual perception of egocentric distance as assessed by triangulation", Journal of Experimental Psychology: Human Perception and Performance, vol. 23(1), 1997, pp. 86-100.
[7] J. Guivant, E. Nebot and S. Baiker, "Autonomous navigation and map building using laser range sensors in outdoor applications", Journal of Robotic Systems, vol. 17, no. 10, 2000, pp. 565-583.
[8] K. Klasing, D. Althoff, D. Wollherr and M. Buss, "Comparison of surface normal estimation methods for range sensing applications", IEEE International Conference on Robotics and Automation (ICRA) 2009, pp. 3206 – 3211.
[9] F. Chaumette and S. Hutchinson, "Visual servoing and visual tracking". Handbook of Robotics, Chapter 24, Springer, 2008.
[10] T. Ringbeck and B. Hagebeuker, "A 3D time of flight camera for object detection", Optical 3D Measurement Techniques, ETH Zurich, 2007.
[11] J. Huang and C.H. Menq, "Automatic data segmentation for geometric feature extraction from unorganized 3-D coordinate points", IEEE Transactions on Robotics and Automation, 2001, pp. 268 – 279.
[12] H. Woo, E. Kang, S. Wang and K. H. Lee, "A new segmentation method for point cloud data", International Journal of Machine Tools and Manufacture, vol. 42, no. 2, 2002, pp. 167-178.
[13] K. Klasing, D. Wollherr, and M. Buss, "Realtime segmentation of range data using continuous nearest neighbors", IEEE International Conference on Robotics and Automation (ICRA), 2009, pp. 2431 – 2436.
[14] H. Badino, D. Huber, Y. Park and T. Kanade, "Fast and accurate computation of surface normals from range images", IEEE International Conference on Robotics and Automation (ICRA), 2011, pp. 3084 – 3091.
[15] N.J. Mitra and A. Nguyen, "Estimating surface normals in noisy point cloud data", Symposium on Computational Geometry (SoCG), 2003, pp. 322 – 328.

[16] D. L. Page, Y. Sun, A. F. Koschan, J. Paik, and M. A. Abidi, "Normal vector voting: Crease detection and curvature estimation on large, noisy meshes", Journal of Graphical Models, vol. 64, 2003, pp. 199 – 229.

[17] D. Ou Yang and H. Yung Feng, "On the normal vector estimation for point cloud data from smooth surfaces", Journal Computer-Aided Design, vol. 37 Issue 10, 2005, pp. 1071 – 1079.

[18] R. Lattuada and J. Raper, "Applications of 3D delaunay triangulation algorithms in geoscientific modelling", 3rd National Conference GIS Research UK, 1995.

[19] R. Poranne, C. Gotsman and D. Keren, "3D surface reconstruction using a generalized distance function", Computer Graphics Forum, vol. 29, no. 8, 2010, pp. 2479–2491.

[20] G. Grudic, "Outdoor path labeling using polynomial mahalanobis distance", Robotics: Science and Systems (RSS), 2006, pp. 4.

[21] J. Iqbal, N.G. Tsagarakis and D.G. Caldwell, "A multi-DOF robotic exoskeleton interface for hand motion assistance", 33rd annual IEEE international conference of Engineering in Medicine and Biology Society (EMBS), Boston, US, 2011, pp. 1575-1678.

[22] J. Iqbal, N.G. Tsagarakis and D.G. Caldwell, "Design of a wearable direct-driven optimized hand exoskeleton device", 4th International Conference on Advances in Computer-Human Interactions (ACHI) 2011, France, pp. 142-146.

[23] J. Iqbal, O.Ahmad and A. Malik, "HEXOSYS II – Towards realization of light mass robotics for the hand", 15th IEEE International Multitopic Conference (INMIC), 2011, pp. 115-119.

[24] J. Iqbal, N.G. Tsagarakis, A.E. Fiorilla and D.G. Caldwell, "A portable rehabilitation device for the hand", 32nd annual IEEE international conference of Engineering in Medicine and Biology Society (EMBS), Buenos Aires, Argentina, 2010, pp. 3694-3697

[25] J. Iqbal, N.G. Tsagarakis and D.G. Caldwell, "A human hand compatible optimised exoskeleton system", IEEE international conference on RObotics and BIOmimetics (ROBIO), China, 2010, pp. 685-690

[26] J. Iqbal, N.G. Tsagarakis, A.E. Fiorilla and D.G. Caldwell, "Design requirements of a hand exoskeleton robotic device", 14th IASTED International Conference on Robotics and Applications (RA), Massachusetts US, 2009, pp. 44-51

[27] J. Iqbal, N.G. Tsagarakis and D.G. Caldwell, "Design optimization of a hand exoskeleton rehabilitation device", proceedings of RSS workshop on understanding the human hand for advancing robotic manipulation, Seattle US, 2009, pp. 44-45.

[28] K. Naveed, J. Iqbal and H. ur Rahman, "Brain controlled human robot interface", IEEE International Conference on Robotics and Artificial Intelligence (ICRAI) 2012, pp. 55-60.

9/3/2013